Bio-Inspired Multiproperty Materials: Strong, Self-Healing, and Transparent Artificial Wood Nanostructures

Rémi Merindol, Seydina Diabang, Olivier Felix, Thierry Roland, Christian Gauthier, Gero Decher

▶ **To cite this version:**

Rémi Merindol, Seydina Diabang, Olivier Felix, Thierry Roland, Christian Gauthier, et al.. Bio-Inspired Multiproperty Materials: Strong, Self-Healing, and Transparent Artificial Wood Nanostructures. ACS Nano, 2015, 9 (2), pp.1127-1136. ⟨10.1021/nn504334u⟩. ⟨hal-04378699⟩

HAL Id: hal-04378699

https://hal.science/hal-04378699v1

Submitted on 25 May 2026

HAL is a multi-disciplinary open access archive for the deposit and dissemination of scientific research documents, whether they are published or not. The documents may come from teaching and research institutions in France or abroad, or from public or private research centers.

L'archive ouverte pluridisciplinaire **HAL**, est destinée au dépôt et à la diffusion de documents scientifiques de niveau recherche, publiés ou non, émanant des établissements d'enseignement et de recherche français ou étrangers, des laboratoires publics ou privés.

Distributed under a Creative Commons CC BY-NC-ND 4.0 - Attribution - Non-commercial use - No Derivative Works - International License

Bio-Inspired Multi-Property Materials: Strong, Self-Healing and Transparent Artificial Wood Nanostructures

Rémi Merindol,[†,§] Seydina Diabang,[†] Olivier Felix,[†,] Thierry Roland,[†,$] Christian Gauthier[†,µ] and Gero Decher[†,§,◊,*]*

[†] CNRS Institut Charles Sadron, 23 rue du Loess, F-67034 Strasbourg, France.

[§] Faculté de Chimie, 1 rue Blaise Pascal, F-67008 Strasbourg, France.

$ INSA de Strasbourg, 24 Bd de la Victoire, F-67084 Strasbourg, France,

µ UFR de Physique, Université de Strasbourg, 4 rue Blaise Pascal, F-67081 Strasbourg, France

[◊] International Center for Frontier Research in Chemistry, 8 allée Gaspard Monge, F-67083 Strasbourg, France

Corresponding Author

* Address correspondence to decher@unistra.fr and olivier.felix@ics-cnrs.unistra.fr

Author Contributions

The manuscript was written through contributions of all authors. All authors have given approval to the final version of the manuscript.

ABSTRACT

Nano-composite films possessing multiple interesting properties (mechanical strength, optical transparency, self-healing and partial biodegradability) are discussed. We used Layer-by-Layer assembly to prepare micron thick wood-inspired films from anionic microfibrillated cellulose and cationic poly(vinyl amine). The film growth was carried out at different pH values for obtaining films of different chemical composition, whereby and as expected, higher pH values led to a higher polycation content and also to 6 times higher film growth increments (from 9 to 55 nm per layer pair). In the pH range from 8 to 11 micron-thick and optically transparent LbL-films are obtained by automated dipping when dried regularly in a stream of air. Films with a size of 10 cm^2 or more can be peeled from flat surfaces, they show tensile strengths up to about 250 MPa and Young's moduli up to about 18 GPa as controlled by the polycation/polyanion ratio of the film. Experiments at different humidities revealed the plasticizing effect of water in the films and allowed to reversibly switch their mechanical properties. Whereas dry films are strong and brittle (Young's modulus: 16 GPa, strain at break 1.7 %), wet films are soft and ductile (Young's modulus: 0.1 GPa, strain at break 49%). Wet film surfaces even amalgamate upon contact to yield mechanically stable junctions. We attribute the switchability of the mechanical properties and the propensity for self-repair to changes in the polycation mobility that are brought about by the plastifying effect of water.

GRAPHICAL TABLE OF CONTENT

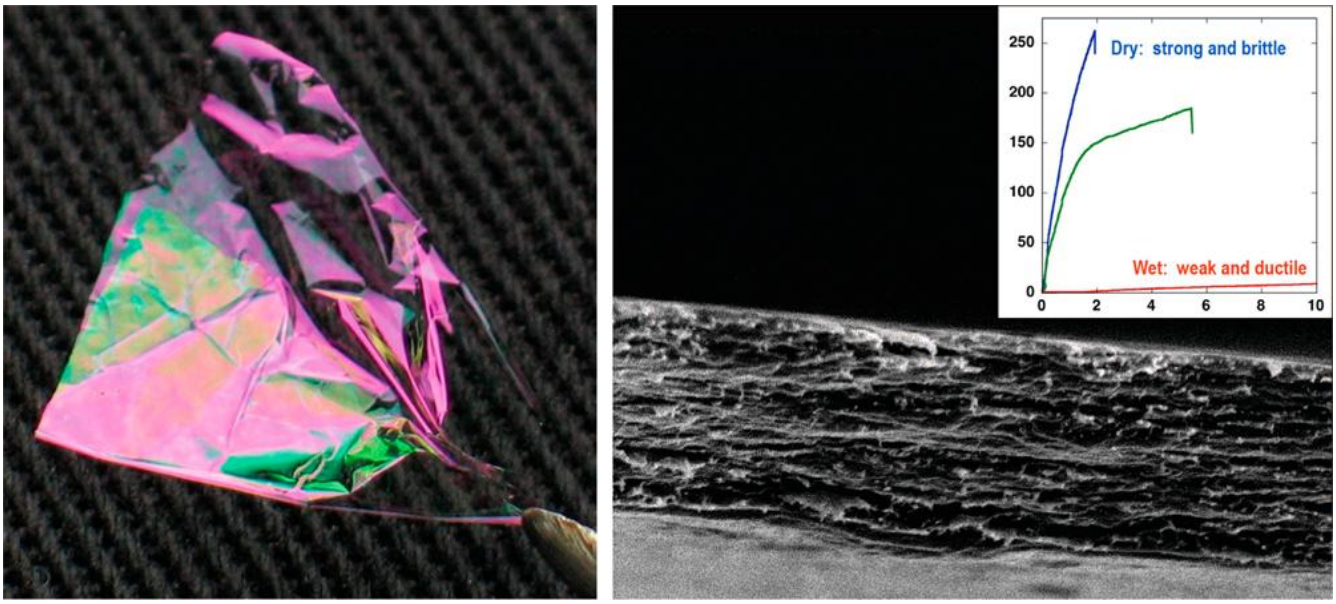

KEYWORDS. Layer-by-Layer assembly · microfibrillated cellulose · artificial wood · bio-inspired nanostructures · multi-property materials · mechanical properties · self-healing · transparent coatings

The great strength of Layer-by-Layer (LbL) assembled films[1] is based on the ease by which multimaterial nano-composites can be prepared and structurally controlled. A classic concept for improving the mechanical properties of a material is by dispersing so-called reinforcing agents in the material. However, such dispersions often have a tendency to de-mix, which strongly decreases their optical transparency and which also degrades the "reinforcing effect" which depends on optimum distances of individual reinforcing objects in the matrix material. Kotov et al. have for example shown that two-material nano-composites with record mechanical strengths can be obtained by LbL-assembly of polymers and clay platelets[2] or carbon nanotubes.[3] The advantage of LbL-assembly for the preparation of nano-composites is that the structure of the composite films is based on the deposition sequence (which determines the layer sequence) and the deposition conditions (which control for example the adsorbed amounts per layer). The fact that LbL-films require the different components in adjacent layers to interact with each other attractively helps to prevent or at least diminish phase separation and de-mixing. Consequently, some LbL-films maintain their structure and properties over several years. On the other hand, the charges in weak polyelectrolytes can be gradually switched on or off by changing the pH of the environment. By doing this the charge density along the polymer backbone can be varied and thus the strength of the interaction with the neighboring counter-polyion can be fine-tuned.[4] We have therefore chosen a reinforcing agent carrying weak anionic groups (carboxyl groups) (anionic microfibrillated cellulose, MFC) in combination with a weak polycation (poly(vinyl amine), PVAm) (Scheme 1) as matrix polymer which is used in the paper industry and which is known to improve for example the dry strength of paper.[5]

The fact that wood is a biodegradable material with excellent mechanical properties controlled by its composition[6] and structure[7] gave rise to the hope that the LbL-assembly of this polyanion/polycation pair would lead to a fiber-reinforced nanocomposite whose mechanical properties could be fine-tuned through a simple variation of the pH during the preparation of the composite material while

maintaining a good control of its nanostructure through the LbL-assembly process. In collaboration with L. Wagberg we had already shown that the combination of anionic MFCs with poly(ethlene imine) leads to LbL-films with good structural control as demonstrated by the observation of optical interference colors that are stable over prolonged periods of time.[8] Such "structural colors" are only observed with objects that are optically homogeneous with respect to their thickness and their refractive index and are therefore also a qualitative indicator for structural homogeneity.

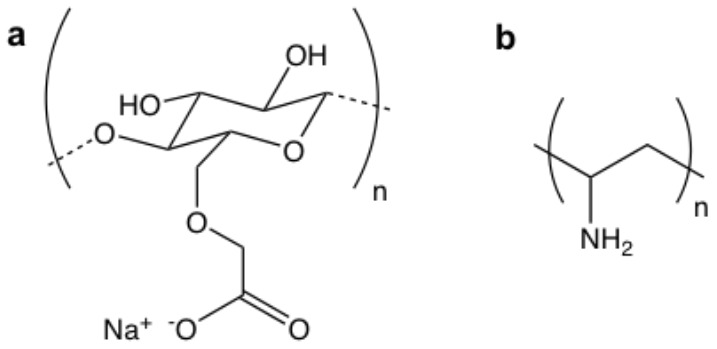

Scheme 1. Chemical structures of anionic microfibrillated cellulose (a) and poly(vinyl amine) (b).

The preparation of artificial wood nanostructures that we introduce here is based on the Layer-by-Layer deposition of MFC and PVAm at different pH on silicon wafers by dipping. As expected, the growth of such films turned out to be sensitive to the pH of PVAm solution that controls the PVAm content. Higher pH values led to a transition from nearly linear to superlinear growth, a higher polycation content and to 6 times higher growth increments (from 9 to 55 nm). Optically transparent thick freestanding films prepared in the pH range from 8 to 11 were peeled from modified silicon wafers and their mechanical properties were studied as a function of the pH and the relative humidity. Higher pH led to higher Young's moduli and lower strains at break while tensile strengths stay in the range of the best MFC-based materials (200-250 MPa). As humidity increases, Young's modulus and

strain of the film decrease while strain at break increases. The switchability of the mechanical properties and the propensity for self-healing could be attributed to changes in the polycation mobility (interaction strength between the building blocks) that are brought about the plastifying effect of water. Such polyelectrolyte mobility in LbL-films was already reported to enable self-healing in water.[9] Strong LbL-assembled films with structural control and self-repair abilities are a new milestone toward high technology applications in the growing field of nanocellulose-based materials.[10,11]

RESULTS AND DISCUSSION

Control of PVAm Content in the Films by the pH. The pH of the PVAm solution was varied from 8 to 11 during construction of the LbL-films while the pH values for the MFC suspension and for the rinsing solution were kept constant at pH = 6.0 ± 0.5 (Figure 1).

As the charge density of the PVAm is reduced with higher pH PVAm is increasingly incorporated into the LbL-film; a 6 layer pair film built at pH = 8 was 35 ± 1 nm thick while a 6 layer pair film built at pH = 11 was 187 ± 10 nm. Simultaneously the growth regime of the film changes from nearly linear to superlinear. This phenomenon, reported for other polyelectrolyte couples,[4,12,13] is related to the decrease of the charge of the PVAm (pKa around 10) with the pH, while the MFCs bearing carboxylic groups (pKa around 4.5) do not see their degree of ionization modified in the studied pH range.[14] As the charge on the PVAm chains decreases the amount of PVAm adsorbing on reference cellulose surfaces increases.[15] At the same time the mobility of the PVAm in the film increases, and the film growth becomes superlinear. In all experiments, we rinsed with pure water (pH = 6.0) to prevent salt crystallization during drying. The solutions of MFC were also kept at a pH of 6 to prevent colloidal destabilization. Under these experimental conditions, we observed a clear effect of the pH on the construction of the films, the superlinear behavior may, have been amplified by the alternation of high and low pH.[16]

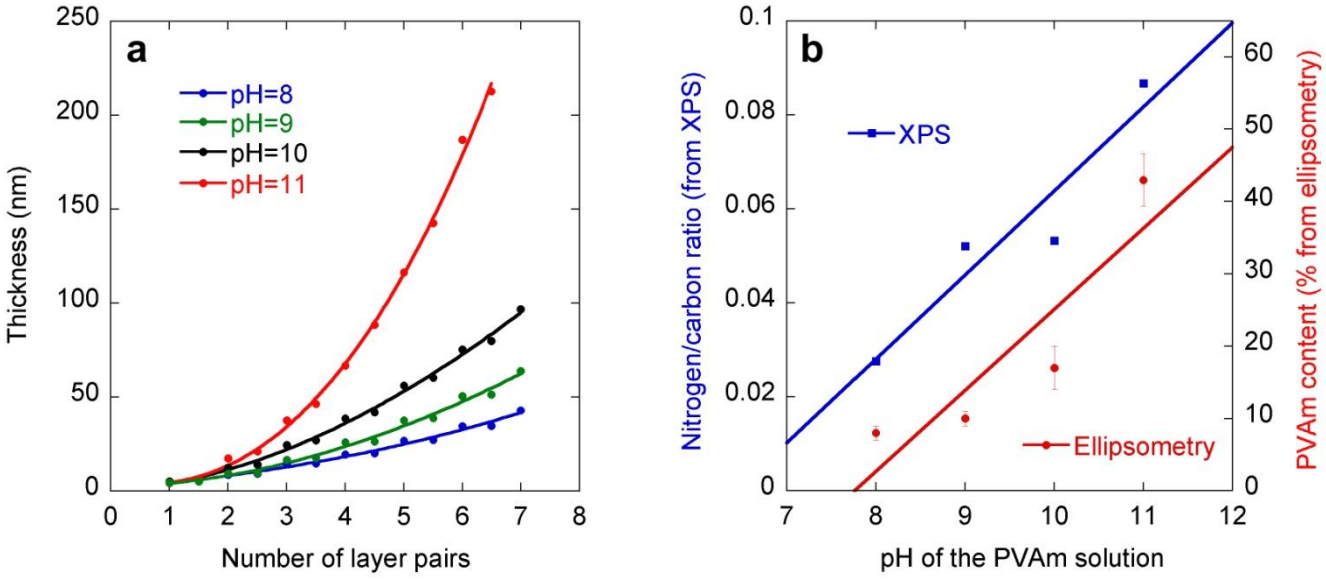

Figure 1. (a) Build-up of LbL-films as a function of the pH of the PVAm solution followed by ellipsometry. Error bars are smaller than the size of the data points. (b) Content of PVAm in the films built at different pH values. (in blue) Ratio of the integral under the N1s and C1s peaks in the XPS spectra of micron thick films with MFC as last layer. (in red) Percentage of the ellipsometric thickness increase for the PVAm layer. Solid lines have no physical meaning and are guide to the eye only.

Ellipsometry also reveals that the amount of PVAm adsorbed in the film during build-up increases with the pH (Figure 1b). This observation is coherent with previously reported results on other films.[17] To corroborate our ellipsometric data, we recorded the X-ray photonelectron spectroscopy (XPS) spectra of similar micron thick films prepared by dipping with MFC as last layer. By increasing the pH of the PVAm solution, the area under the peak of the 1s orbital of nitrogen increases as compared to the area under the peak of the 1s orbital of carbon, revealing that the content of nitrogen on the surface is multiplied by a factor of about 3 as the pH is raised from 8 to 11. Morphology of $(PVAm/MFC)_8$ films built at pH = 8 and 11 by dipping is shown in Supporting Information (Figure S1). Note that the effect

of this controlled variation of the film composition with respect to PVAm (energy dissipating matrix) and MFC (nano-reinforcing component) on mechanical properties of such films will be studied later on in the manuscript.

Construction and Characterization of Thick LbL-Films. Our equipment for mechanical tests (tensile strength) was designed for a force range of 0.05 to 2.5 N and requires, therefore, to work with films with a thickness in the micron range. The preparation of homogeneous films in this thickness range required several optimizations, especially at the different pH values. Another challenge is the preparation of thick freestanding LbL-films. The use of hydrofluoric acid to dissolve the glass substrate[2] is not possible here as it would damage cellulose fibers in the film. Another way to detach a thin film from its support consists in surface modification of a silicon wafer with fluorinated or alkyl chains allowing film construction with similar growth as compared to classic activated silicon wafers.[18] In our case, however, the construction of thick film on such modified substrates led to the formation of crack patterns on the surface of the film. At pH = 8 the first cracks appeared at a film thickness of about 600 nm making the mechanical tests impossible. The apparition of cracks is probably due to the shrinking of the film upon drying in combination with poor adhesion on the silicon substrate. We noticed that the cracking of the film was pH sensitive; increasing the pH lowered significantly the number of cracks. Apparently, as the amount of polymer in the film increases, the stress generated by drying decreases, this probably also explains why previously reported films containing about 20 % of poly(ethylene imine) did not crack.[18]

The construction of multilayers directly on hydrophobic silicon wafer has already been reported for LbL-films composed of clays and poly(vinyl alcohol).[19] In this study, we used one layer pair of this clay-based system to enhance the adhesion of our film on the hydrophobic substrate. After deposition of this adhesion layer it became possible to build micron thick films without cracks. We believe that this combination of hydrophobic substrate and adhesion layer could be widely used for the general

preparation of freestanding LbL-films and likely for other type of films as well. Hydrophobic substrates covered with clay present a surface very similar to the one of activated silicon wafer traditionally used in LbL-deposition. Films deposited on top of theses substrates can then be easily removed using tape or tweezers due to the weak adhesion of the film on the substrate.

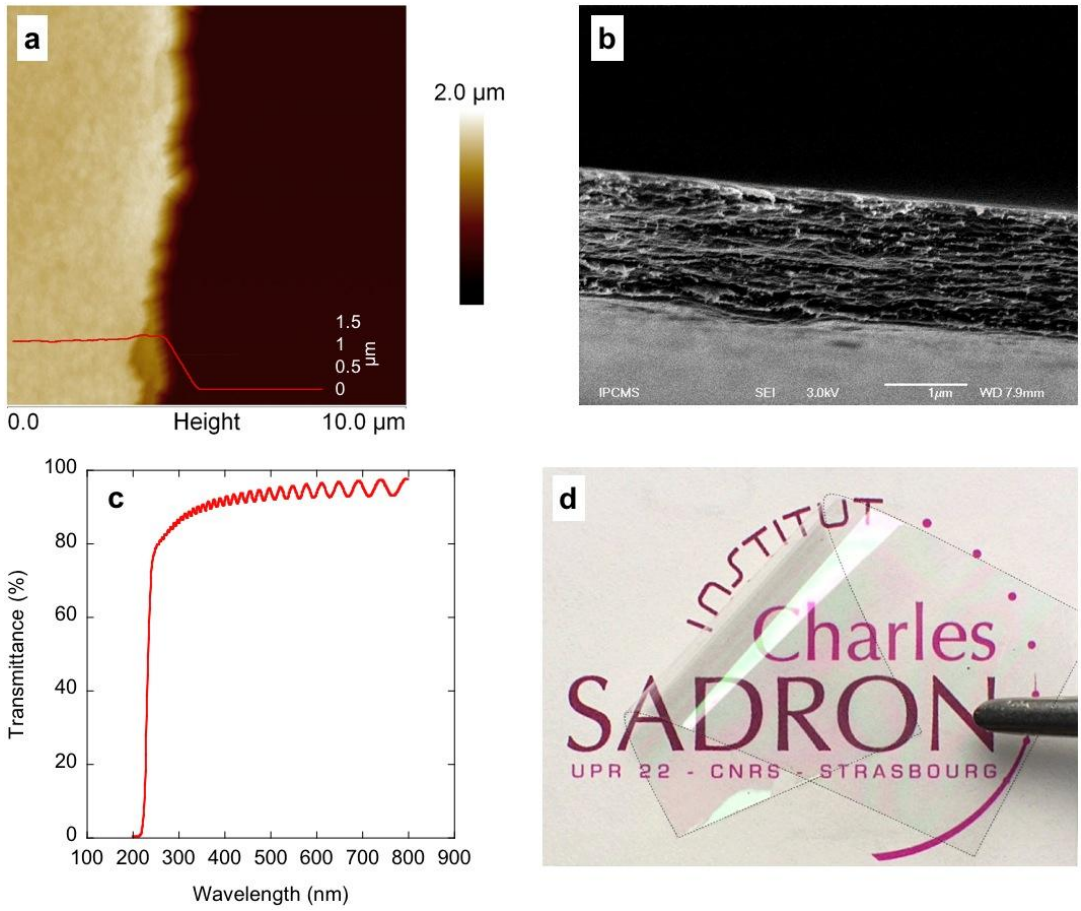

Figure 2. (a) AFM image and profile (insight in red) of the edge of a $(PVAm/MFC)_{70}$ film built from a PVAm solution at pH = 9 resting on a silicon wafer (brown background on the right). The profile was taken roughly on the middle of the image. A film thickness of 1.1 µm is observed by AFM and is in agreement with that measured by spectroscopic ellipsometry (1.1 ± 0.1 µm). (b) Cross section SEM image of a $(PVAm/MFC)_{30}$ film built from a PVAm solution at pH = 11. A film thickness of 1.6 µm is observed by SEM and corresponds to that measured by spectroscopic ellipsometry (1.6 ± 0.1 µm). (c)

UV-Vis spectrum of a freestanding $(PVAm/MFC)_{75}$ film built from a PVAm solution at pH = 10. The film thickness obtained by spectroscopic ellipsometry is 3.4 ± 0.1 µm. (d) Optical photograph of a $(PVAm/MFC)_{60}$ film built from a PVAm solution at pH = 10.5. The film thickness measured by spectroscopic ellipsometry is 3.8 ± 0.1 µm. The edges of the film are marked with a dotted line to facilitate the observation of the film borders.

The scanning electron microscopy (SEM) image and the profile obtained by atomic force microscopy (AFM) (Figures 2a and 2b) are representative of the microscopic aspect of the different freestanding LbL-films obtained. In plane orientation of cellulose micro-fibrils in the film can be clearly seen by SEM using a secondary electrons detector. All methods used confirm that films prepared are uniformly thick, homogeneous and rather smooth. In order to obtain smooth edges for microscopy the film were notched and carefully torn. The use of a scalpel gave in some cases rough edges that prevented accurate thickness measurements. The AFM profile shows a bump near the edge, which is caused by accumulation of material during cutting. One can also observe on the edge at the bottom of the image an intermediate step on the edge of the film, which is typical of layered materials. Thicknesses measured by scanning electron microscopy and spectroscopic ellipsometry are similar, this underlines the accuracy of the model used for spectroscopic ellipsometry and carried out with a constant refractive index equal to 1.55 for the entire film.

The UV-visible transmittance of a $(PVAm/MFC)_{75}$ freestanding film was recorded in the spectral range 200 and 800 nm (Figure 2c). The film shows a high transparency in the visible spectrum with over 85% transmittance, while it strongly absorbs UV below 250 nm. Contrary to films prepared by vacuum filtration[20] the film do not require any additional treatment to be transparent. The UV visible spectrum also displays typical Fabry-Perrot fringes confirming the excellent homogeneity of the film

thickness and refractive index.[21] The optical photography (Figure 2d) confirms the high transparency of the film. One can also distinguish shades of green and pink on the picture, these colors come from interferences and are typically observed for thin films with uniform thickness and low surface roughness. These films can be easily manipulated and folded without breaking.

Mechanical Characterization of the Freestanding Films. The mechanical properties of the $(PVAm/MFC)_n$ films built from different PVAm solutions were systematically studied varying the ratio of polymer to nano-reinforcing component. In order to get comparable values for the different films the number of layer pairs was adjusted to have a similar total thickness for all the films (from 1.0 to 1.6 microns).

The mechanical characteristics obtained for these materials (Table 1) (with strength up to 290 MPa in some cases) are in the range of the best MFC based material[20,22] and are approaching the strongest LBL-based materials (400 MPa).[2] We found that the Young's modulus of the film was sensitive to the pH of PVAm solution during film construction; at pH = 8 and 9 the modulus was around 12 GPa while at pH = 10 and 11 we found a modulus around 17 GPa.

pH	Number of layer pairs	Thickness (μm)	Young's Modulus (GPa)	Stress at break (MPa)	Strain at break (%)
8	150	1.35 (± 0.01)	12.1 (± 1.8)	206 (± 66)	4.7 (± 3.1)
9	70	1.12 (± 0.05)	11.9 (± 1.1)	209 (± 19)	8.9 (± 2.6)
10	30	1.02 (± 0.03)	17.7 (± 0.6)	197 (± 27)	2.5 (± 1.8)
11	30	1.65 (± 0.07)	16.5 (± 1.5)	141 (± 43)	0.9 (± 0.4)

Table 1. Mechanical characteristics of micron thick films built from PVAm solutions at pH ranging from 8 to 11.

We attributed this increase to a better reinforcing efficiency of the embedded MFCs as the content of PVAm increases. Similarly films built at pH = 8 and 9 had a lower yield strength than the film built at pH = 10, and the film built at pH = 11 always broke before yielding (Figure 3).

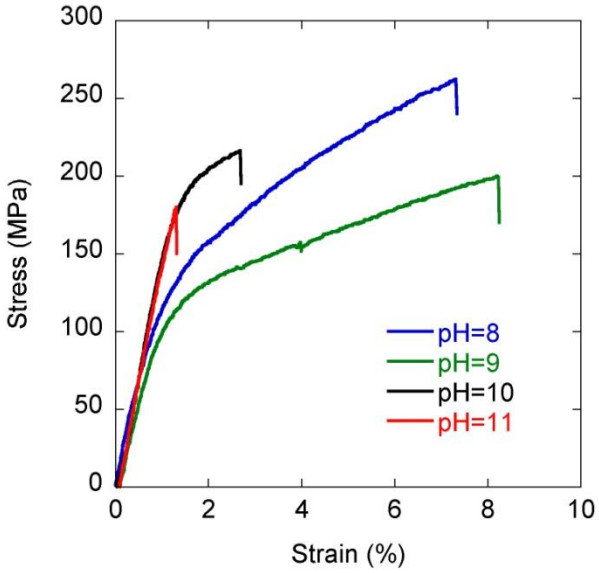

Figure 3. Typical stress-strain curves obtained for micron thick $(PVAm/MFC)_n$ films built from PVAm solutions at pH ranging from 8 to 11.

When the content in PVAm increases there are less weak fiber/fiber interactions and more stronger fiber/PVAm interactions, therefore the Young's modulus and the yield strength increase. At pH = 10 an optimum composition seems to be reached with a high Young's modulus, high strength and fast growth. However the best values in terms of strength (290 MPa or 235 MPa) were obtained for films built at low pH probably due to higher content of MFC responsible of the higher toughness. The relatively large error bars obtained for these measurements are due to the difficulty to obtain perfectly smooth edges during sample preparation that leads to premature breaking of the film. In any case, the general profile of the tensile curves obtained for films built at one given pH is characteristic. Similar

mechanical tests on multilayers containing cationic microfibrillated cellulose and poly(acrylic acid) deposited at pH = 3 displayed similar mechanical properties with strength reaching 250 MPa.

The strength and modulus of the different films are higher than what was found by Wägberg et al.[8] for freestanding MFC-based films. They attributed the low strength of their films to the absence of humidity. We addressed this problem by measuring the mechanical properties of the films in different humidity conditions.

Using Water as a Plasticizing Agent. Water is known to have a strong plasticizing effect on polyelectrolyte complexes.[23] Therefore, we studied the effect of relative humidity (RH) on the mechanical properties of a film built at pH = 10 (Figure 4).

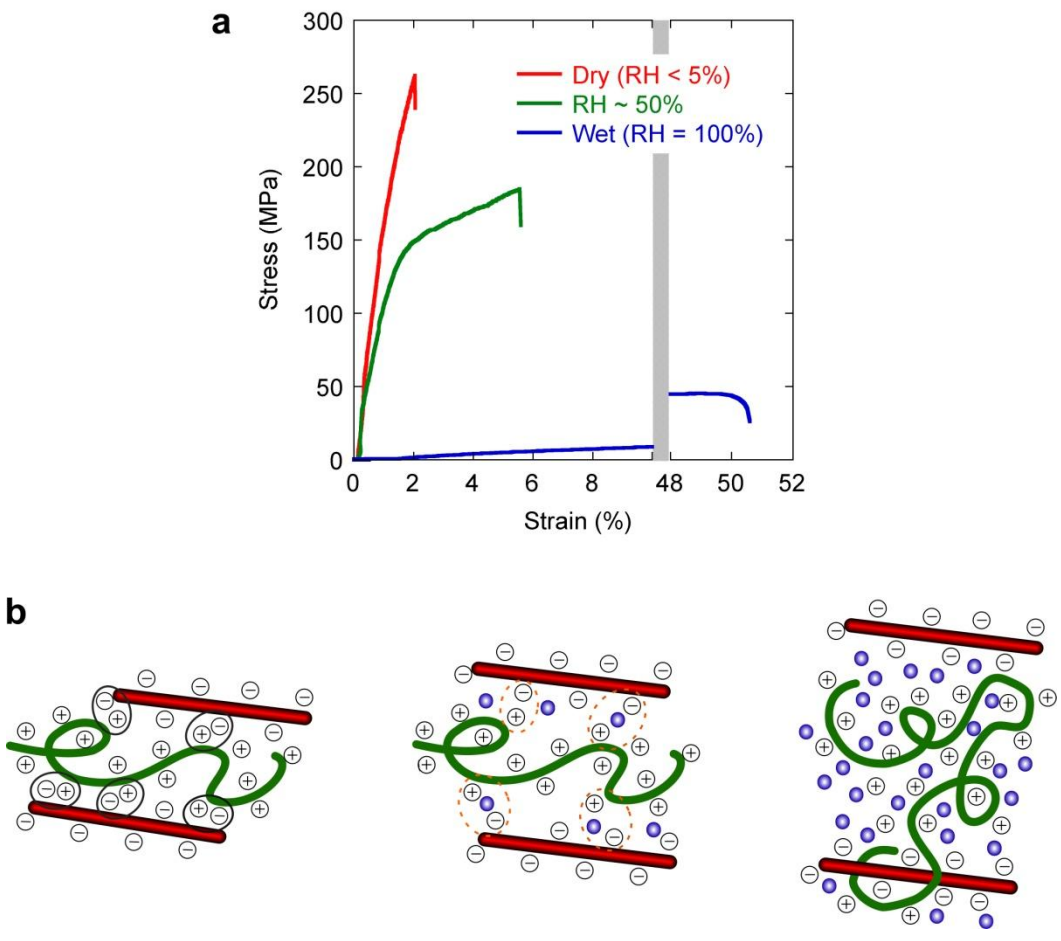

Figure 4. (a) Typical stress-strain curves obtained for $(PVAm/MFC)_n$ thick films (3.4 ± 0.1 μm) built from PVAm solution at pH = 10 in various humidity conditions. Note that the x-axis was interupted between 10 and 48% for clarity. (b) Simplified molecular sketch of the effect of hydration on the interactions between MFC and PVAm. The green lines represent PVAm, the red sticks correspond to MFC and the blue dots represent the water molecules in the film, + and - symbols are representing respectively pending ammonium and carboxylates groups (counter ions have been omitted for clarity).

The general trend of humidity can be clearly seen on the stress-strain curves (Figure 4a). As humidity increases, strength and Young's modulus of the film decrease while the strain at break increases. This effect can be mostly attributed to the nature of the interactions in the material (Figure 4b).

Humidity	Young's Modulus (GPa)	Stress at break (MPa)	Strain at break (%)
< 5 %	16 (± 3)	237(± 31)	1.7 (± 0.4)
~ 50 %	12 (± 2)	174 (± 20)	3.3 (± 2.2)
Wet (100%)	0.12 (± 0.01)	46 (± 11)	49 (± 8)

Table 2. Mechanical characteristics of thick $(PVAm/MFC)_n$ films (3.4 ± 0.1 μm) built from PVAm solution at pH = 10 in various humidity conditions.

At low RH, there is very little water in the film, the electrostatic interactions among the CNF fibers,29 among the polymer chains and between the fibers and the PVAm, are strong, and the PVAm is rigid. This leads to a very strong composite, reaching the strengths of the best MFC-based materials with low maximal strain and no plastic deformation. Compared to previously reported MFC-containing LbL-films[18] these films have higher Young's modulus and strength. We attributed this to the strong bonding

of PVAm to the cellulose. [24] Long linear polymers are also known to reach higher strength than dendrimers as they reach higher degrees of entanglements for similar molecular weight.[25] The humidity conditions at which we performed the mechanical tests are also slightly higher (~ 3%) than those used by Wägberg and coworkers (~ 0%) but a lower humidity appears to increase the maximal strength.

At ambient conditions (RH ~ 50%), the film absorbs some water. As a consequence the electrostatic interactions and the hydrogen bonds between MFC and PVAm decrease and the poly(vinyl amine) is partially plastified. Surprisingly the Young's modulus is weakly affected (Table 2). This is compatible with theories for macro-composites with high aspect ratio fibers.[25] However recent experiments on LbL films suggested a different behavior.[26,27] This difference could be explained by the polycation used, poly(vinyl amine) in our case, that is known to bring wet strength to paper,[24] while poly(ethylene imine) might be more sensitive to humidity. Another explanation for the differences in these results, are the techniques used, buckling mechanics and tensile experiments might lead to different results when applied to lamellar composites.[28]

At ambient humidity conditions the films yield around 150 MPa and reach strains up to 6%. The plastic deformation can be explained according to shear-lag theories[29] with sliding at the interface between the fibers and the PVAm or plastic deformation of the PVAm. Both phenomena would be promoted by the increase of humidity as water can either plastify PVAm or screen the electrostatic interactions between the fiber and the polymer matrix.

In wet conditions (RH = 100%), the film swells and the electrostatic interactions and hydrogen bonds between MFC and PVAm are greatly decreased and the PVAm highly hydrated allowing rearrangements and diffusion in the film. Consequently the Young's modulus decreases to 120 MPa and the maximal stress decreases to a quarter of its room humidity value. On the other side the maximal strain increases to 50%. The elastic modulus and maximal strain are calculated using the film thickness measured in the dry state; this makes difficult the comparison with other cellulose hydrogels.[30,31]

Interestingly heating the dry film for 12 hours at 120ºC before mechanical test doubled the strength and Young's modulus of the wet film but didn't impact significantly the properties at other humidity conditions. The wet strength relies mostly on covalent bonds (such as amide bonds created during thermal treatment), while in the dry state electrostatic interactions and hydrogen bonds are sufficient to reach high strength.

One notices a lower strength and Young's modulus for this 3.4 µm film than for the 1.0 µm thick film built at pH = 10 (Table 1 and 2). It appeared that there was a decrease of the pH of the PVAm solution during deposition. After 30 layer pairs the pH of the PVAm solution was 9.8 while after 75 layer pairs it was 9.3. This explains why the mechanical properties of the thicker film are located between the properties of the film built at pH = 10 and at pH = 9. Based on this observation, the conclusions on the changes of mechanical properties with humidity remain valid.

During our investigations, we observed that the films had tendency to stick to themselves after immersion in water. Some cases of self-repairing LbL materials showing superlinear growth have already been reported in the litterature.[9] Thus, we tried a simple self-repairing experiment where the edges of two wet films were superposed. This led to the production of a freestanding film. Then, we carried out tensile tests on the repaired films and surprisingly all the samples broke outside the repaired region (Figure 5b). The stress at break obtained for repaired films was 157 ± 33 MPa that is comparable to the 174 ± 20 MPa obtained for native films. On the deformation mapping obtained by digital image correlation (Figure 5c) it appears that the part of the film adhering together are deforming much less than the rest of the film. The lower deformation in this region reveals a proper healing; the film behaves as if it was a continuous film with a region twice as thick in the middle. We do not observe regions of high and low deformation that would appear if the films were sliding or partially de-laminating. The red parts at the bottom of the images come from artifacts in the calculation of deformation at the limits of the area of interest known as edge effects. These self-repairing tests are not

a quantitative representation of the self-repairing ability of these materials, but an edge to edge contact was impossible for such thin films and the cellulose micro-fibrils prevent lateral diffusion for scratch healing.

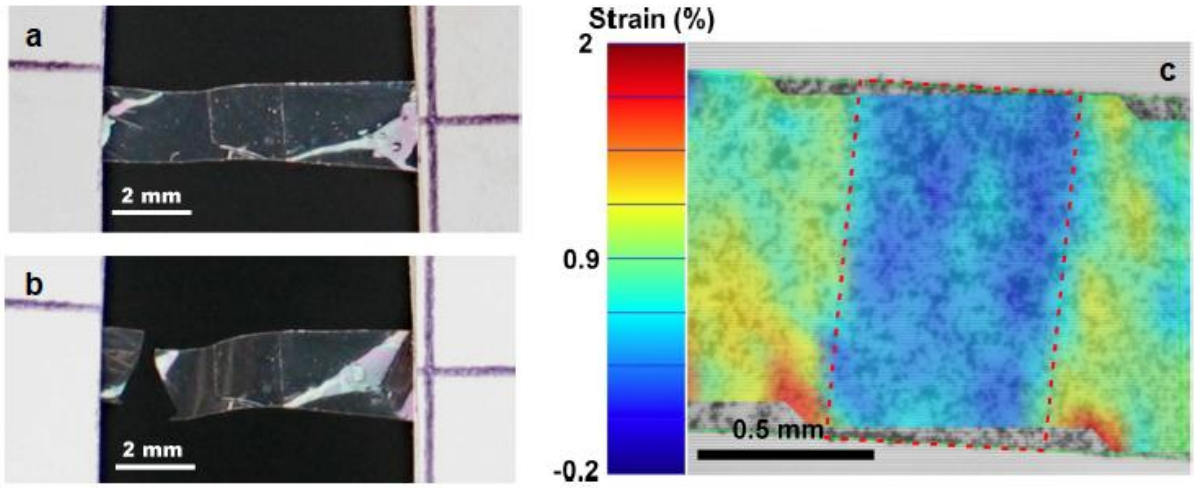

Figure 5. Image of a self-repaired film before (a) and after (b) pulling on it. (c) Visualization of the deformation of a repaired film by image correlation. The image extracted from the video (grey scale) displays the film with black patterns coming from printer toner deposited on it. The colors added by the correlation software, show in blue low deformation regions, and in orange high deformations. The overlap region is outlined in dashed red.

The repairing properties observed in wet conditions are enabled by the mobility of the polymer chains in the multilayer in presence of water. Composite hydrogels showing somewhat similar behavior have been described.[32,33] Films build with poly(acrylic acid) and cationic microfibrilated cellulose showed similar self-healing behavior when the pH of the poly(acrylic acid) solution was adjusted to 2-3.

SUMMARY AND CONCLUSIONS

This study demonstrates that LbL assembly is capable of producing thick transparent artificial wood nanostructures composed of MFC and PVAm with tunable mechanical performances and a propensity for self-healing. The mechanical properties of such nanocomposites films were tuned through the pH of the PVAm solution during film build-up and the relative humidity of the surrounding environment during mechanical tests. Chemical composition, growth regime and thickness of the MFC-based LbL-films were controlled by the pH of the PVAm solution. Higher pH values led to higher PVAm content and to 6 times higher film growth increments (from 9 nm at pH = 8 to 55 nm at pH = 11). These films showed tensile strengths up to 250 MPa and Young's moduli up to 18 GPa as controlled by the polycation/polyanion ratio of the film.

External stimuli (changes in humidity) were used to switch the mechanical performance of films prepared at pH 10. While dry films are strong and brittle (tensile strength around 240 MPa, Young's modulus of 16 GPa and strain at break of 1.7 %) wet films are soft and ductile (tensile strength around 50 MPa, Young's modulus 0.1 GPa and strain at break of 49 %). These reversible mechanical property changes are attributed to the plasticizing effect of water controlling the polycation mobility in the films. The latter even leads to the self-healing of wet films upon contact, amalgamated junctions between the two film surfaces show remarkable mechanical stability.

METHODS

Materials. Microfibrillated cellulose (MFC) was obtained from Innventia AB (Stockholm, Sweden) as a pulp containing 2.5% of fibers in water. The pulp was mechanically dispersed in Milli-Q water (Milli-Q Gradient system, Millipore, Molsheim, France) to obtain a suspension at 2 g/L and sonicated with tip sonicator (Vibra cell 75042 from Bioblock Scientific, Illkirch, France) for one hour at 20% of

amplitude. The resulting suspension was centrifugated for 3 hours at 5000 rpm (centrifuge 4K10 with Rotor Nr 12254 from Sigma, Lyon, France), and the resulting supernatant was used as deposition solution after filtration on cotton wool. Typical concentration was in the range of 0.9 g/L as determined from dry mass measurement.

Poly(vinyl amine) (trade name LUPAMIN 9095, PVAm, 20% in Water, $\overline{M_w}$ ≈ 340000 g/mol, more than 90% hydrolysed) was freely provided by BASF and diluted in water to obtain a 1 g/L solution. The pH of the solutions was adjusted using a 0.5 M sodium hydroxide solution.

Poly(vinyl alcohol) (trade name Moviol 10-98, PVAl, $\overline{M_w}$ ≈ 61000 g/mol, 98% of hydrolysis) was purchased from Sigma-Aldrich (Lyon, France) and dissolved at 5 g/L in Milli-Q water at 80°C and filtered over cotton wool.

Clay (EMX 2039 Sodium Montmorillonite) was freely provided by Clariant Produkte GmbH (Moosburg, Germany) and suspended in Milli-Q water by stirring 10 g of clay in 1 L of water for 3 days. The non exfoliated clays were removed by centrifugation for 3 hours at 5000 rpm (centrifuge 4K10 with Rotor Nr 12254 from Sigma, Lyon, France) and the supernatant was re-diluted with Milli-Q water to obtain a 2.5 g/L solution (estimated from dry mass).

Sodium hydroxide pellets (> 97%) were purchased from Sigma-Aldrich (Lyon, France) and diluted in Milli-Q water to obtain a 0.5 M solution.

Silicon wafer (200 mm in diameter) were purchased from Wafernet Inc. (San José, CA) and cut in 3 x 10 cm dimensions.

Octadecyltrichlorosilane (OTS, > 97%) was purchased from Acros-Organics (Illkirch, France). Toluene (> 99.9%) was obtained from VWR Chemical (Strasbourg, France). Ethanol absolute anhydrous (> 99.9%) was obtained from Carlos Erba Reagents (Peypin, France).

Substrate Preparation. The silicon wafer (Si wafer) slides were cleaned using ethanol (10 min in ultrasound bath) and Milli-Q water (10 min in ultrasound bath) and dried using compressed air flow. Clean silicon wafers were activated for 3 min in a Plasma Cleaner (Harrick Plasma, Ithaca, NY) on medium intensity.

LbL-Deposition. The substrate was dipped for 5 min in the PVAm solution followed by three rinsing steps of 1 min. The substrate was then dried with compressed air (typically 1 min). The same steps were applied for the deposition of MFC. This procedure consisted of one deposition cycle (layer pair) and was repeated until the desired thickness was reached.

Surface Modification of Si Wafer. The activated silicon wafers were dipped in freshly prepared solution of Octadecyltrichlorosilane 0.1% in toluene for one hour. Then the modified substrates were cleaned with fresh toluene, ethanol and Milli-Q water and rubbed with dust free cloth (Ko-ton, Chicopee Europe, AA Cuijk, The Netherlands). After surface modification, typically the thickness increased from 1.8 nm for activated silicon wafers to 4.5 nm (ellipsometry measurements).

Adhesive Layer. For silicon wafer modified with octadecyltrichlorosilane, an adhesive first layer pair was needed in order to prevent film cracking and tearing off. The clean surface modified silicon wafers were dipped in PVAl solution for 5 min followed by three rinsing steps of 1 min. After drying with compressed air, the substrate was dipped in clay solution for 5 min followed by three rinsing steps of 1 min, and drying with compressed air. The substrate was then used directly for construction of the multilayer.

Automated Deposition. Preparation of the micron thick $(PVAm/MFC)_n$ multilayers was performed using a home made dipping robot, consisting of three motorized arms (x,y,z directions), a drying station, an interface from ISEL (Houdan, France) and a Labview home made program. The deposition was done according to the procedure described above in the section LbL-deposition.

Ellipsometry. For thin films (up to 3000Å), the thickness measurements were done using a PLASMOS SD 2300 operating at a wavelength of 632.8nm and with an angle of 70°. The refractive index was set at n = 1.465 and assumed to be constant. Each data point is an average of 10 measurements at random positions on the wafer. This procedure leads to slightly inexact absolute thicknesses values but it allows a quick determination of the thickness and sufficient precision for the comparison of the build-up and homogeneity of the different films reported here.

For thicker films a spectroscopic ellipsometer SENpro (SENTECH Instruments GmbH, Berlin Germany) was used. The film was modeled as a single layer with a constant refractive index of 1.55. This value was coherent with thicknesses observed by AFM and SEM and did not appear to change with the pH used during film deposition. Each thickness recorded is the average of five measurements done along the length of the sample.

Atomic Force Microscopy (AFM). Tapping mode atomic force microscopy was performed on an AFM Multimode from Bruker Nano Surface (Palaiseau, France) with the controller Nanoscope IV from Veeco (Mannheim, Germany) and non coated silicon cantilevers (resonance frequency 300kHz, resonance constant of 40 N/m, and radius below 10 nm). Phase and height modes were recorded simultaneously using a constant scan rate of 1.3 Hz with a resolution of 512 x 512 pixels.

In order to measure the film edges without breaking the supporting silicon wafer, a small piece of the freestanding film was cut and transferred on an activated silicon wafer. The transfer was done with the help of a drop of water on which the film is initially deposited, after drying it with compressed air the film laid flat on the surface.

Scanning Electron Microscopy (SEM). Films were observed with a scanning electron microscope (JEOL 6700, JEOL SAS, Croissy-sur-Seine, France) equipped with a field emission gun (SEM-FEG) at an accelerating voltage of 3 KV. The imaging was done with the SEI detector collecting secondary electrons. Before imaging the multilayer films were notched and carefully torn with tweezers in order

to obtain a sharp edge. Samples were glued vertically with carbon tape and about 5 nm of conductive carbon were evaporated on the surface before imaging.

UV-Visible Spectroscopy. Transmission spectra were recorded directly on the freestanding films with a Cary 5000 spectrometer from Agilent Technologies France SAS (Les Ulis, France).

X-ray photoelectron spectroscopy (XPS). Photoemission spectra of the film were measured on thick multilayers deposited on a silicon wafer. The measurements were performed on a Multilab 2000 (Thermo) spectrometer equipped with Al Kα anode (hν = 1486.6 eV). The nitrogen to carbon ratio have been calculated using the sensitivity factors, as determined by Scofield[34] directly on the nitrogen and carbon peaks respectively at 399.7eV and 285.2eV.

Sample Preparation for Mechanical tests. The LbL-films were cut using a scalpel blade (regularly changed to prevent tearing of the film). Typically stripes (~ 1.5 mm wide and 15 mm long) were cut directly from the silicon wafer. Each stripe was then suspended, with double faced tape, in a U-shaped support consisting of a 25 x 20 mm piece of paper with a 5 x 10 mm gap in the middle (Supporting Information, Figure S2a). The paper support allows easier handling and positioning of the sample in the tensile test machine.

We created a pattern on the surface of the film in order to follow the true deformation by image correlation during the tensile test (Supporting Information, Figure S2b). The pattern was made using black printer toner that electrostatically attach to the surface of the film. The dry toner was loaded on a brush and flicked on the film from 2 cm distance, the excess was then removed using a gentle blow of compressed air.

Mechanical Tests. A custom made tensile test machine equipped with a 2.5 N load cell included in a thermal and climatic chamber was used. The film support was fixed at the two jaws of the machine. After cutting the paper support, the film was the only bridge between the two parts of the instrument.

The tensile tests were performed at constant strain rate of 0.01 mm/s, at room temperature and the force applied on the film was continuously recorded until rupture of the film occurred.

Digital Image Correlation. Because of the compliance of the machine and deformation of the tape used to fix the sample, direct measurement of the true strain of the film by the machine was impossible. Therefore, the true strain was obtained using digital image correlation.[35,36] This technique tracks the displacement of a random grey scale pattern on a sequence of images. Each image is subdivided and a correlation algorithm is used to match the sub-divisions between two images. The strain is then obtained by derivation of the displacement.

In our case a 0.5 Mega pixel camera was recording the tests at 6 images/second with an image size of 1.86 x 1.40 mm. Typically a sequence of 60 images regularly spaced were extracted from the video and imported into the digital image correlation software, CORRELISTC. Each image was subdivided into elements of 32 pixels and reference image for the correlation algorithm was actualized every 5 images. The deformation was then averaged from 81 points (arranged on a 9 x 9 grid) and reported as true strain in the stress-strain curves. The use of relatively soft tape is compensating eventual misalignment and allows reducing partially the error on the maximal strain.

Control of Humidity. Tests run at RH ~ 50% were performed at room conditions (actual humidity was between 45 and 55%, no modification was observed within theses values). All samples were equilibrated at room conditions for at least 24 hours before measurement.

Tests run at RH < 5% were carried out in a confined environment under a flow of filtered compressed air with a RH in the range of 2-3%. All samples were equilibrated before the tests for at least 24 hours in a desiccator cabinet with freshly activated silica gel.

For tests done in wet conditions (RH = 100%) a drop of water was deposited on the upper surface of the film 5 min prior to testing (deposition 30 min prior to testing did not make any significant difference). In these tests the patterning used for the measurement of the deformation was deposited on

the lower surface to prevent washing off with water. These films were kept at room conditions before measurement.

Self-Repairing Experiments. A large piece (~ 20 x 20 mm) is cut in a freshly prepared film. Then, the piece of film is dipped into Milli-Q water and deposited on the silicon wafer next to the rest of the initial film with a small overlap (0.6 to 2 mm). The contact was made between the two upper surfaces of the film in order to prevent interference from the adhesion layer of the film (it however did not seem to make any significant difference when the back side was put in contact with the front side). The repaired film was then gently dried with flow of compressed air. Stripes (~ 1.5mm) of films were then cut with scissors perpendicularly to the initial cut and tested with the same mechanical set-up as described previously.

Supporting Information Available. AFM images of $(PVAm/MFC)_8$ films built on silicon wafer with a PVAm solution at pH = 8 (a) and at pH = 11 (b), optical images of a thick LbL film placed in a U-shaped support and after staining with powder toner. This material is available free of charge via the Internet at http://pubs.acs.org.

Acknowledgement. We gratefully acknowledge support from the Ministère de l'Enseignement Supérieur et de la Recherche, France, the Centre National de la Recherche Scientifique (CNRS), France, the International Center for Frontier Research in Chemistry, France and the Institut Universitaire de France, France. All authors are indebted to Cedric Leuvrey (IPCMS, France) for SEM images, to Christophe Contal (ICS, France) for AFM tutorial and discussions, to Innventia AB (Sweden) for providing microfibrillated cellulose, to BASF (Germany) for providing poly(vinyl amine) and to Lars Wågberg (KTH Royal Institute of Technology, Sweden) for fruitful discussions.

Abbreviations. AFM, atomic force microscopy; LbL, Layer-by-Layer; MFC, microfibrillated cellulose; OTS, Octadecyltrichlorosilane; PVAm, poly(vinyl amine); RH, relative humidity; Rq, surface roughness; SEM, scanning electron microscopy; XPS, X-ray photoelectron spectroscopy.

REFERENCES AND NOTES

1. Decher, G., Fuzzy Nanoassemblies: Toward Layered Polymeric Multicomposites. *Science* **1997,** *277* (5330), 1232-1237.
2. Podsiadlo, P.; Kaushik, A. K.; Arruda, E. M.; Waas, A. M.; Shim, B. S.; Xu, J.; Nandivada, H.; Pumplin, B. G.; Lahann, J.; Ramamoorthy, A.; Kotov, N. A., Ultrastrong and Stiff Layered Polymer Nanocomposites. *Science* **2007,** *318* (5847), 80-83.
3. Shim, B. S.; Zhu, J.; Jan, E.; Critchley, K.; Ho, S. S.; Podsiadlo, P.; Sun, K.; Kotov, N. A., Multiparameter Structural Optimization of Single-Walled Carbon Nanotube Composites: Toward Record Strength, Stiffness, and Toughness. *ACS Nano* **2009,** *3* (7), 1711-1722.
4. Bieker, P.; Schönhoff, M., Linear and Exponential Growth Regimes of Multilayers of Weak Polyelectrolytes in Dependence on pH. *Macromolecules* **2010,** *43* (11), 5052-5059.
5. Lorencak, P.; Stange, A.; Niessner, M.; Esser, A., Polyvinylamine-A New Polymer for Increasing Paper Strength. *Wochenblatt Für Papierfabrikation* **2000,** *128* (1-2), 14-18.
6. Gibson, L. J., The hierarchical Structure and Mechanics of Plant Materials. *J. R. Soc. Interface* **2012,** *9* (76), 2749-2766.
7. Lichtenegger, H.; Reiterer, A.; Stanzl-Tschegg, S. E.; Fratzl, P., Variation of Cellulose Microfibril Angles in Softwoods and Hardwoods - A Possible Strategy of Mechanical Optimization. *J. Struct. Biol.* **1999,** *128* (3), 257-269.
8. Wagberg, L.; Decher, G.; Norgren, M.; Lindstroem, T.; Ankerfors, M.; Axnaes, K., The Build-up of Polyelectrolyte Multilayers of Microfibrillated Cellulose and Cationic polyelectrolytes. *Langmuir* **2008,** *24* (3), 784-795.
9. Wang, X.; Liu, F.; Zheng, X.; Sun, J., Water-Enabled Self-Healing of Polyelectrolyte Multilayer Coatings. *Angew. Chem. Int. Ed.* **2011,** *50* (48), 11378-11381.
10. Klemm, D.; Kramer, F.; Moritz, S.; Lindstrom, T.; Ankerfors, M.; Gray, D.; Dorris, A., Nanocelluloses: A New Family of Nature-Based Materials. *Angew. Chem. Int. Ed.* **2011,** *50* (24), 5438-5466.
11. Siro, I.; Plackett, D., Microfibrillated Cellulose and New Nanocomposite Materials: a Review. *Cellulose* **2010,** *17* (3), 459-494.
12. Fu, J. H.; Ji, J.; Shen, L. Y.; Kueller, A.; Rosenhahn, A.; Shen, J. C.; Grunze, M., pH-Amplified Exponential Growth Multilayers: A Facile Method to Develop Hierarchical Micro- and Nanostructured Surfaces. *Langmuir* **2009,** *25* (2), 672-675.
13. Choi, J.; Rubner, M. F., Influence of the Degree of Ionization on Weak Polyelectrolyte Multilayer Assembly. *Macromolecules* **2005,** *38* (1), 116-124.
14. Feng, X.; Pelton, R.; Leduc, M.; Champ, S., Colloidal Complexes from Poly(vinyl amine) and Carboxymethyl Cellulose Mixtures. *Langmuir* **2007,** *23* (6), 2970-2976.
15. Geffroy, C.; Labeau, M. P.; Wong, K.; Cabane, B.; Stuart, M. A. C., Kinetics of Adsorption of Polyvinylamine onto Cellulose. *Colloids and Surfaces A* **2000,** *172* (1-3), 47-56.
16. Peng, C. Q.; Thio, Y. S.; Gerhardt, R. A.; Ambaye, H.; Lauter, V., pH-Promoted Exponential Layer-by-Layer Assembly of Bicomponent Polyelectrolyte/Nanoparticle Multilayers. *Chem. Mater.* **2011,** *23* (20), 4548-4556.
17. Yoo, D.; Shiratori, S. S.; Rubner, M. F., Controlling Bilayer Composition and Surface Wettability of Sequentially Adsorbed Multilayers of Weak Polyelectrolytes. *Macromolecules* **1998,** *31* (13), 4309-4318.

18. Karabulut, E.; Wagberg, L., Design and Characterization of Cellulose Nanofibril-based Freestanding Films Prepared by Layer-by-Layer Deposition Technique. *Soft Matter* **2011,** *7* (7), 3467-3474.
19. Patro, T. U.; Wagner, H. D., Layer-by-Layer Assembled PVA/Laponite Multilayer Free-standing films and their Mechanical and Thermal Properties. *Nanotechnology* **2011,** *22* (45).
20. Nogi, M.; Iwamoto, S.; Nakagaito, A. N.; Yano, H., Optically Transparent Nanofiber Paper. *Adv. Mater.* **2009,** *21* (16), 1595.
21. Guan, Y.; Yang, S.; Zhang, Y.; Xu, J.; Han, C. C.; Kotov, N. A., Fabry-Perot Fringes and Their Application To Study the Film Growth, Chain Rearrangement, and Erosion of Hydrogen-Bonded PVPON/PAA Films. *J. of Phys. Chem. B* **2006,** *110* (27), 13484-13490.
22. Henriksson, M.; Berglund, L. A.; Isaksson, P.; Lindstrom, T.; Nishino, T., Cellulose Nanopaper Structures of High toughness. *Biomacromolecules* **2008,** *9* (6), 1579-1585.
23. Hariri, H. H.; Lehaf, A. M.; Schlenoff, J. B., Mechanical Properties of Osmotically Stressed Polyelectrolyte Complexes and Multilayers: Water as a Plasticizer. *Macromolecules* **2012,** *45* (23), 9364-9372.
24. Feng, X.; Pouw, K.; Leung, V.; Pelton, R., Adhesion of Colloidal Polyelectrolyte Complexes to Wet Cellulose. *Biomacromolecules* **2007,** *8* (7), 2161-2166.
25. Landel, R. F.; Nielsen, L. E., *Mechanical Properties of Polymers and Composites, Second Edition*. Taylor & Francis: 1993.
26. Johansson, E.; Wagberg, L., Tailoring the Mechanical Properties of Starch-containing Layer-by-Layer Films. *Colloids and Surfaces A* **2012,** *394*, 14-22.
27. Cranston, E. D.; Eita, M.; Johansson, E.; Netrval, J.; Salajkova, M.; Arwin, H.; Wagberg, L., Determination of Young's Modulus for Nanofibrillated Cellulose Multilayer Thin Films Using Buckling Mechanics. *Biomacromolecules* **2011,** *12* (4), 961-969.
28. Chung, J. Y.; Nolte, A. J.; Stafford, C. M., Surface Wrinkling: A Versatile Platform for Measuring Thin-Film Properties. *Adv. Mater.* **2011,** *23* (3), 349-368.
29. Bonderer, L. J.; Studart, A. R.; Gauckler, L. J., Bioinspired design and assembly of platelet reinforced polymer films. *Science* **2008,** *319* (5866), 1069-1073.
30. Abe, K.; Yano, H., Cellulose Nanofiber-based Hydrogels with High Mechanical Strength. *Cellulose* **2012,** *19* (6), 1907-1912.
31. Way, A. E.; Hsu, L.; Shanmuganathan, K.; Weder, C.; Rowan, S. J., pH-Responsive Cellulose Nanocrystal Gels and Nanocomposites. *ACS Macro Lett.* **2012,** *1* (8), 1001-1006.
32. Haraguchi, K.; Uyama, K.; Tanimoto, H., Self-healing in Nanocomposite Hydrogels. *Macromol. Rapid Commun.* **2011,** *32* (16), 1253-1258.
33. Wang, Q.; Mynar, J. L.; Yoshida, M.; Lee, E.; Lee, M.; Okuro, K.; Kinbara, K.; Aida, T., High-Water-Content Mouldable Hydrogels by Mixing Clay and a Dendritic Molecular Binder. *Nature* **2010,** *463* (7279), 339-343.
34. Scofield, J. H., Hartree-Slater Subshell Photoionization Cross-Sections at 1254 and 1487 eV. *J. Electron. Spectrosc. Relat. Phenom.* **1976,** *8* (2), 129-137.
35. Chu, T. C.; Ranson, W. F.; Sutton, M. A.; Peters, W. H., Application of Digital-Image-Correlation Technique to Experimental Mechanics. *Exp. Mech.* **1985,** *25* (3), 232-244.
36. Hild, F.; Roux, S., Digital Image Correlation: From Displacement Measurement to Identification of Elastic Properties - A Review. *Strain* **2006,** *42* (2), 69-80.